

Probabilistic characteristics of narrow-band long wave run-up onshore

Sergey Gurbatov¹⁾ and Efim Pelinovsky^{2,3)}

1) National Research University – Lobachevsky State University, Nizhny Novgorod, Russia

2) National Research University – Higher School of Economics, Moscow, Russia

3) Institute of Applied Physics, Nizhny Novgorod, Russia

Abstract

The run-up of random long wave ensemble (swell, storm surge and tsunami) on the constant-slope beach is studied in the framework of the nonlinear shallow-water theory in the approximation of non-breaking waves. If the incident wave approaches the shore from the deepest water, run-up characteristics can be found in two stages: at the first stage, linear equations are solved and the wave characteristics at the fixed (undisturbed) shoreline are found, and, at the second stage, the nonlinear dynamics of the moving shoreline is studied by means of the Riemann (nonlinear) transformation of linear solutions. In the paper, detailed results are obtained for quasi-harmonic (narrow-band) waves with random amplitude and phase. It is shown that the probabilistic characteristics of the run-up extremes can be found from the linear theory, while the same ones of the moving shoreline - from the nonlinear theory. The role of wave breaking due to large-amplitude outliers is discussed, so that it becomes necessary to consider wave ensembles with non-Gaussian statistics within the framework of the analytical theory of non-breaking waves. The basic formulas for calculating the probabilistic characteristics of the moving shoreline and its velocity through the incident wave characteristics are given. They can be used for estimates of the flooding zone characteristics in marine natural hazards.

Keywords: tsunami, storm surge, long wave run-up, Carrier-Greenspan transform, statistical characteristics

1. Introduction

The flooded area size, the water flow depth and its speed on the coast, the coastal topography characteristics determine the consequences of marine natural disasters on the coast. The catastrophic events of recent years are well known, when tsunami waves and storm surges caused significant damage on the coast and people's death. It is worth saying that only in 2018 two catastrophic tsunamis occurred in Indonesia, leading to the death of several thousand people (on Sulawesi Island in September and in the Sunda Strait in December). The calculations of the coastal flooding due to tsunamis and storm surges are mainly carried out within the framework of nonlinear shallow-water equations, taking into account the variable roughness coefficient for various areas of the coastal zone (Kaiser et al, 2011; Choi et al, 2012). The characteristics of the

38 coastal destruction are determined either by using fragility curves (Macabuag et al, 2016; Park et
39 al, 2017) or by using a direct calculation of the tsunami forces (Qi et al, 2014; Ozer et al, 2015a,
40 b; Kian et al, 2016; Xiong et al., 2019).

41 The computation accuracy was tested on a series of benchmarks, including the idealized
42 problem of the wave run-up onto the impenetrable slope of a constant gradient without friction
43 (Synolakis et al, 2008). The nonlinear shallow water equations for the bottom geometry of this
44 kind are linearized by using the hodograph (Legendre) transformations. This step makes it possible
45 to obtain a number of exact solutions describing the run-up on the coast. This approach, first
46 suggested by Carrier and Greenspan (1958), was later on used to analyze the run-up of single and
47 periodic waves of various shapes (Synolakis, 1987; Pelinovsky and Mazova, 1992; Carrier, 1995;
48 Carrier et al, 2003; Tinti and Toniti, 2005; Madsen and Fuhrman, 2008; Madsen and Schaffer,
49 2010; Antuano and Brocchini, 2008, 2010; Didenkulova, 2009; Dobrokhotov et al, 2015; Aydin
50 and Kanoglu, 2017). Moreover, such approach made it possible to determine the conditions for the
51 wave breaking. The latter means the presence of steep fronts (the gradient catastrophe) within the
52 hyperbolic shallow water equation framework. The Carrier-Greenspan transformation was further
53 generalized for the case of waves in an inclined channel of an arbitrary variable cross-section
54 (Rybkin et al, 2013; Pedersen, 2016; Shimozone, 2016; Anderson et al, 2017; Raz et al, 2018). In
55 a number of practical cases, its use proves to be more efficient than the direct numerical
56 computation within the 2D shallow water equation framework (Harris et al, 2015, 2016).

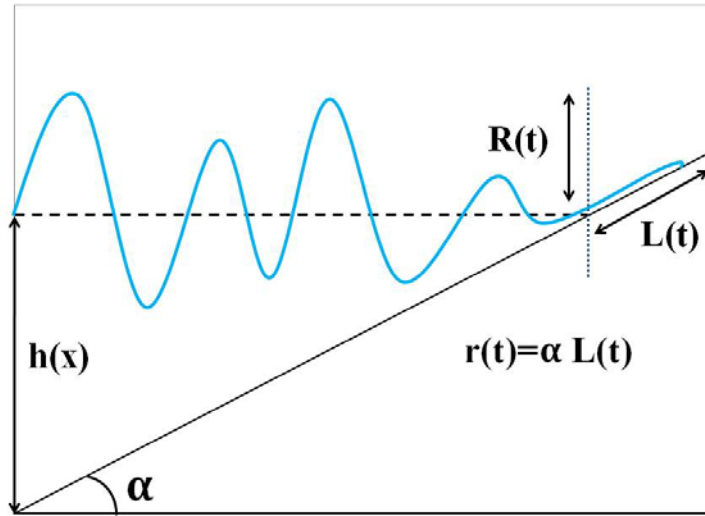
57 Due to the bathymetry variability and shoreline complexity, diffraction and scattering effects
58 lead to an irregular shape of the waves approaching the coast. Moreover, very often the leading
59 wave is not the maximum one. Such typical tsunami wave records on tide-gauges are well known
60 and are not shown here. It is applied even more to swell waves, which in some cases approach the
61 coast without breaking (Huntley et al, 1977; Hughes et al, 2010). As a result, the statistical wave
62 theory can be applied to such records and nonlinear shallow water equations in the random function
63 class can be solved. This approach was used to describe the statistical moments of the long wave
64 run-up characteristics in (Didenkulova et al, 2008, 2010, 2011). Special laboratory experiments
65 were also conducted on irregular wave run-up on a flat slope, the results of which are not very well
66 described by theoretical dependencies (Denissenko et al, 2011, 2013). As for the field data, we are
67 acquainted with two papers: (Huntley et al, 1977; Hughes et al, 2010), where the statistical
68 characteristics of the moving shoreline on two Canadian and one Australian beaches were
69 calculated. They confirmed the fact that the wave process on the coast is not Gaussian. In our
70 opinion, the main problem in the theoretical model of describing the irregular wave run-up on the
71 shore is associated with the use of two hypotheses: 1) the small amplitude wave field (in the linear

72 problem) is Gaussian; 2) waves run-up on the shore without breaking. It is obvious, however, that
73 in the nonlinear wave field some broken waves can always be present. They affect the distribution
74 function tails and, thus, the statistical moments of the run-up characteristics as well.

75 The connection of the run-up parameters at the nonlinear stage with the linear field at a
76 fixed point is described either in a parametric form or implicitly in the nonlinear equation
77 (Didenkulova et al., 2010). This does not allow using the standard methods of random processes.
78 At the same time, it is known, that this implicit equation is equivalent to a partial first-order
79 differential equation (PDE), that is, to the simple (the Riemann wave) equation (Rudenko and
80 Soluyan, 1977). In statistical problems, this equation arises in nonlinear acoustics. This equation
81 or its generalization, the nonlinear diffusion equation called the Burgers equation (Burgers et al,
82 1974) is the model equation in the hydrodynamic turbulence theory (Frisch, 1995). It should be
83 noted that for the one-dimensional Burgers turbulence, as well as its three-dimensional version,
84 used for the model description of the large-scale Universe structure (Gurbatov et al, 2012), it is
85 possible to give an almost comprehensive statistical description for certain initial conditions
86 (Gurbatov et al, 1991, 1997, 2011; Gurbatov and Saichev, 1993; Molchanov et al, 1995; Frisch,
87 1995; Woyczynski, 1998; Frisch and Bec, 2001; Bec and Khanin, 2007). In particular, the single-
88 point and the two-point probability distributions of the velocity field and even the N -point
89 probability distributions and, accordingly, the multi-point moment functions were found. This
90 partially allows using a mathematical approach developed in statistical nonlinear acoustics. An
91 experimental study of the nonlinear evolution of random quasi-monochromatic waves and the
92 probability distributions and spectra analysis have been carried out in acoustics more than once.
93 They confirmed theoretical conclusions; see, for example (Gurbatov et al, 2018, 2019).

94 This paper is devoted to the analytical study of the probabilistic characteristics of the long
95 narrow-band wave run-up on the coast. Section 2 gives the basic equations of nonlinear shallow
96 water theory and the Carrier-Greenspan transformation, with the latter making it possible to
97 linearize the nonlinear equations. Section 3 describes the moving shoreline dynamics when the
98 deterministic sine wave approaches the slope. The probability characteristics of the deformed sine
99 oscillations of the moving shoreline with a random phase are described in Section 4. Section 5
100 contains the probabilistic characteristics on the vertical displacement of the moving shoreline if
101 the incident narrow-band wave has a random amplitude and phase. The discussion of the wave
102 breaking effects and their influence on the distribution of the run-up characteristics is given in
103 Section 6. The results obtained are summarized in Section 7.

104



106

107

Fig. 1. The problem geometry

108

109 Here we will consider the classical formulation of the problem of a long wave run-up on the
 110 constant-gradient slope in an ideal fluid (Fig. 1). The wave is one-dimensional and propagates
 111 along the x -axis directed onshore. The basin depth is a linear depth function: $h(x) = -\alpha x$, where
 112 α is the inclination angle tangent and point $x = 0$ corresponds to a fixed unperturbed water
 113 shoreline. $L(t)$ and $r(t)$ describe the horizontal and vertical displacement of the moving shoreline,
 114 and $R(t)$ is the water level oscillations at $x = 0$. The bottom and the shore are assumed impenetrable.
 115 The long wave dynamics is described by nonlinear shallow water equations:

$$116 \quad \frac{\partial u}{\partial t} + u \frac{\partial u}{\partial x} + g \frac{\partial \eta}{\partial x} = 0, \quad (2.1)$$

$$117 \quad \frac{\partial \eta}{\partial t} + \frac{\partial}{\partial x} [(-\alpha x + \eta)u] = 0. \quad (2.2)$$

118 Here, $\eta(x,t)$ is the free surface elevation above the undisturbed water level, and $u(x,t)$ is the depth-
 119 averaged flow velocity (within the shallow water theory, the flow velocity is the same on all
 120 horizons), and g is the gravity acceleration. Obviously, after introducing the total depth

$$121 \quad H(x,t) = -\alpha x + \eta(x,t), \quad (2.3)$$

122 equations (2.1) and (2.2) are a hyperbolic system with constant coefficients. This fact makes it
 123 possible to transform the system into a linear equation one by using a hodograph (Legendre)

124 transformation, which was done in the pioneering work by Carrier and Greenspan in 1958. As a
 125 result, the wave field is described by a linear wave equation in the ‘cylindrical’ coordinate system

$$126 \quad \frac{\partial^2 \Phi}{\partial \lambda^2} - \frac{\partial^2 \Phi}{\partial \sigma^2} - \frac{1}{\sigma} \frac{\partial \Phi}{\partial \sigma} = 0, \quad (2.4)$$

127 and all variables are expressed in terms of an auxiliary wave function $\Phi(\sigma, \lambda)$ using explicit
 128 formulas

$$129 \quad \eta = \frac{1}{2g} \left(\frac{\partial \Phi}{\partial \lambda} - u^2 \right), \quad (2.5)$$

$$130 \quad u = \frac{1}{\sigma} \frac{\partial \Phi}{\partial \sigma}, \quad (2.6)$$

$$131 \quad x = \frac{1}{2\alpha g} \left(\frac{\partial \Phi}{\partial \lambda} - u^2 - \frac{\sigma^2}{2} \right), \quad (2.7)$$

$$132 \quad t = \frac{1}{\alpha g} (\lambda - u). \quad (2.8)$$

133 It should be noted that the variable σ is proportional to the total water depth.

$$134 \quad \sigma = 2\sqrt{gH} = 2\sqrt{g(-\alpha x + \eta)}, \quad (2.9)$$

135 so, the wave equation (2.4) is solved on the semi-axis $\sigma \geq 0$, and this coordinate plays the radius
 136 role in the cylindrical coordinate system. We would like to emphasize that the point $\sigma = 0$
 137 corresponds to a moving shoreline, and therefore, the original problem, solved in the area with an
 138 unknown boundary, is reduced to the fixed area problem.

139 It is important to note that the hodograph transformation is valid if the Jacobian
 140 transformation is non-zero

$$141 \quad J = \frac{\partial(x, t)}{\partial(\sigma, \lambda)} \neq 0. \quad (2.10)$$

142 It is the case when a gradient catastrophe, identified in the framework of the shallow-water theory
 143 with the wave breaking, does not occur. The necessary condition for the wave breaking absence is
 144 the boundedness and smoothness of all solutions; this question will be discussed further on.

145 We will assume that the wave approaches the coast from the area far from the shoreline (
 146 $x \rightarrow -\infty$), where the wave is linear. Then it is obvious that the function $\Phi(\sigma, \lambda)$ can be completely
 147 found from the linear theory. The difficulty in finding the wave field in the near-shoreline area is

148 due to the implicit transformation of the coordinates (x, t) to (σ, λ) . However, for the most
 149 interesting point of the moving shoreline $\sigma = 0$ (its dynamics determines the size of the flooded
 150 area on the coast) all the formulas become explicit. In particular, from (2.5) and (2.6) follows

$$151 \quad r(t) = R \left[t + \frac{u(t)}{\alpha g} \right] - \frac{u(t)^2}{2g}, \quad (2.11)$$

$$152 \quad u(t) = U \left[t + \frac{u(t)}{\alpha g} \right], \quad (2.12)$$

153 where $r(t)$ and $u(t)$ are the vertical displacement of the moving shoreline and its speed, and the
 154 functions $R(t)$ and $U(t)$ determine the field characteristics at the fixed point ($x = 0$) from the linear
 155 theory

$$156 \quad R(t) = \frac{1}{2g} \frac{\partial \Phi(\sigma = 0, \lambda)}{\partial \lambda} \Big|_{\lambda = \alpha g t}, \quad U(t) = \frac{1}{\sigma} \frac{\partial \Phi(\sigma, \lambda)}{\partial \sigma} \Big|_{\sigma = 0, \lambda = \alpha g t}. \quad (2.13)$$

157 Then we add the obvious kinematic relations for the vertical displacement and velocity of the last
 158 sea point along the slope.

$$159 \quad u(t) = \frac{1}{\alpha} \frac{dr(t)}{dt}, \quad U(t) = \frac{1}{\alpha} \frac{dR(t)}{dt}. \quad (2.14)$$

160 Let us note that the formula (2.12) is identical to the so-called Riemann wave or a simple
 161 wave in a nonlinear non-dispersive medium (in particular, in nonlinear acoustics), if we consider
 162 the parameter $1/\alpha g$ to be a ‘coordinate’; see, for example, (Rudenko and Soluyan, 1977, Gurbatov
 163 et al, 1991, 2011). Moreover, the formula (2.13) describes the integral over the Riemann wave.
 164 This analogy proves to be very useful when transferring the already known results in the wave
 165 nonlinear theory to the run-up characteristics described by the formulas (2.11) and (2.12).

166 Detailed calculations of the long wave run-up on the coast were carried out repeatedly; see,
 167 for example (Carrier and Greenspan, 1958; Synolakis, 1987; Pelinovsky and Mazova, 1992; Tinti
 168 and Toniti, 2005; Madsen and Fuhrman, 2008; Madsen and Schaffer, 2010; Antuano and
 169 Brocchini, 2008, 2010; Didenkulova, 2009; Dobrokhotoev et al, 2015; Aydin and Kanoglu, 2017).

170 It is worth mentioning that the nonlinear time transformation in (2.11) and (2.12) leads to
 171 the shoreline oscillation distortion in comparison with the linear theory predictions. So, for large
 172 amplitudes the wave shape becomes multi-valued (broken). The first moment of the wave breaking
 173 on the shoreline (the gradient catastrophe) is easily found from (2.12) by calculating the first
 174 derivative of the moving shoreline velocity

175
$$\frac{du}{dt} = \frac{dU/dt}{1 - \frac{dU/dt}{\alpha g}}, \quad (2.15)$$

176 from it follows the wave breaking condition

177
$$Br = \frac{\max(dU/dt)}{\alpha g} = \frac{\max(d^2R/dt^2)}{\alpha^2 g} = 1, \quad (2.16)$$

178 where we have introduced the breaking parameter Br to designate the left-hand side in (2.16),
 179 which characterizes the nonlinear wave properties on the shoreline. The condition (2.16) can be
 180 given a physical meaning, that the breaking occurs when the last sea particle acceleration (
 181 $\alpha^{-1}d^2R/dt^2$) exceeds the component of the gravity acceleration along the shoreline ($g\alpha$). As
 182 shown in (Didenkulova, 2009), the condition (2.16) coincides with (2.10) for Jacobian. It is
 183 important to emphasize that the breaking condition is unequivocally found through solving the
 184 linear problem of the wave run-up on the shore. It is determined only by the particle acceleration
 185 value on the shoreline; but it is not determined separately by the shoreline displacement or its
 186 velocity.

187 The similar Carrier – Greenspan transformation is obtained for waves in narrow inclined
 188 channels, fjords, and bays (Rybkin et al, 2013; Pedersen, 2016; Anderson et al, 2017; Raz et al,
 189 2018); only the wave equation (2.4) and relations (2.5) - (2.8) change. However, the moving
 190 shoreline dynamics is still described by equations (2.11) and (2.12), valid for arbitrary cross-
 191 section channels.

192

193 **3. The moving shoreline dynamics at an initially monochromatic wave run-up**

194 The monochromatic wave run-up on a flat slope by using the Carrier – Greenspan
 195 transformation has been studied in a number of papers cited above. Let us reproduce here the main
 196 features of the moving shoreline dynamics necessary for us to draw the statistical description
 197 further on. Mathematically, the monochromatic wave run-up is described by an elementary
 198 solution of the equation (2.4)

199
$$\Phi(\sigma, \lambda) = QJ_0(l\sigma) \cos(l\lambda), \quad (3.1)$$

200 where Q and l are arbitrary constants, and J_0 is the zero-order Bessel function. Far from the
 201 shoreline ($\sigma \rightarrow \infty$) the Bessel function decreases, so the wave function Φ becomes small. In this
 202 case, in (2.5) - (2.8) one can use approximate expressions (the ‘linear’ Carrier – Greenspan
 203 transformation)

204
$$\eta = \frac{1}{2g} \frac{\partial \Phi}{\partial \lambda}, \quad u = \frac{1}{\sigma} \frac{\partial \Phi}{\partial \sigma}, \quad x = -\frac{\sigma^2}{4\alpha g}, \quad t = \frac{\lambda}{\alpha g}, \quad (3.2)$$

205 and, using the asymptotic representation for the Bessel function, reduce (3.1) to the expression for
 206 the water surface displacement

207
$$\eta(x,t) = a(x) \left\{ \sin \left[\omega \left(t - \int \frac{dx}{\sqrt{gh(x)}} \right) \right] - \frac{\pi}{4} \right\} + \sin \left[\omega \left(t + \int \frac{dx}{\sqrt{gh(x)}} \right) + \frac{\pi}{4} \right], \quad (3.3)$$

208 where

209
$$a(x) = \frac{Q}{2g} \sqrt{\frac{l}{\pi \sqrt{gh(x)}}}, \quad \omega = gl\alpha. \quad (3.4)$$

210 The wave field away from the shoreline is a superposition of two waves of the same frequency
 211 and a variable amplitude $a(x)$, which together form a standing wave. It immediately shows that
 212 the wave amplitude varies with depth according to the Green law ($h^{-1/4}$), as it should be far from
 213 the coast. The same asymptotic result follows from the exact solution of linear shallow water
 214 equations.

215
$$\eta(x,t) = R_0 J_0 \left(\sqrt{\frac{4\omega^2 |x|}{g\alpha}} \right) \sin(\omega t), \quad (3.5)$$

216 where R_0 is the wave amplitude at the fixed shoreline ($x = 0$), identified with the maximum run-
 217 up height in the linear theory. By connecting (3.4) and (3.5), we obtain the formula for the run-up
 218 height obtained through the incident wave amplitude far from the coast

219
$$\frac{R_0}{a(x)} = \sqrt{\frac{2\omega}{\alpha}} \sqrt{\frac{h(x)}{g}}. \quad (3.6)$$

220 The formula (3.6) allows working further with the run-up height R_0 instead of the wave amplitude
 221 far from the coast $a(x)$. This run-up height will be considered as the given value. Having
 222 determined Q and l through the incident wave parameters, we can calculate the run-up
 223 characteristics in the nonlinear theory, considering the limit of the formula (3.1) with $\sigma \rightarrow 0$ and
 224 using the Carrier – Greenspan transformation formulas (2.5) - (2.8). The moving shoreline
 225 movement is determined by the parametric dependence

226
$$t = \frac{\lambda}{\alpha g} - \frac{\omega R_0}{\alpha^2 g} \cos \left(\frac{\omega \lambda}{\alpha g} \right), \quad (3.7)$$

227
$$r = R_0 \sin \left(\frac{\omega \lambda}{\alpha g} \right) - \frac{\omega^2 R_0^2}{2\alpha^2 g} \cos^2 \left(\frac{\omega \lambda}{\alpha g} \right). \quad (3.8)$$

228 It is convenient to introduce dimensionless variables

$$229 \quad z = \frac{r}{R_0}, \quad \tau = \omega t, \quad \varphi = \frac{\omega \lambda}{\alpha g}, \quad (3.9)$$

230 and calculate the breaking parameter

$$231 \quad Br = \frac{\omega^2 R_0}{\alpha^2 g}, \quad (3.10)$$

232 so the formulas (3.7) and (3.8) are finally rewritten in the form

$$233 \quad \tau = \varphi - Br \cos(\varphi), \quad (3.11)$$

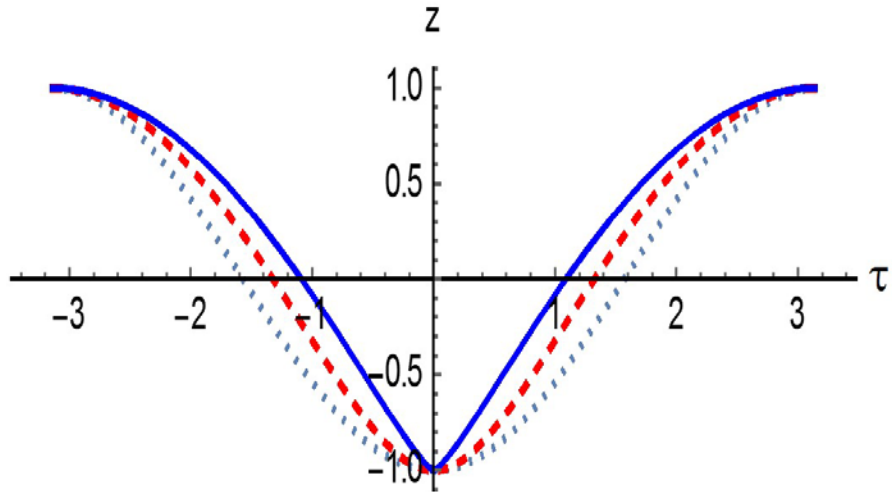
$$234 \quad z = \sin(\varphi) - \frac{Br}{2} \cos^2(\varphi), \quad (3.12)$$

235 what is another expression for the formulas (2.11) and (2.12), if we take

$$236 \quad R(t) = R_0 \sin(\omega t), \quad (3.13)$$

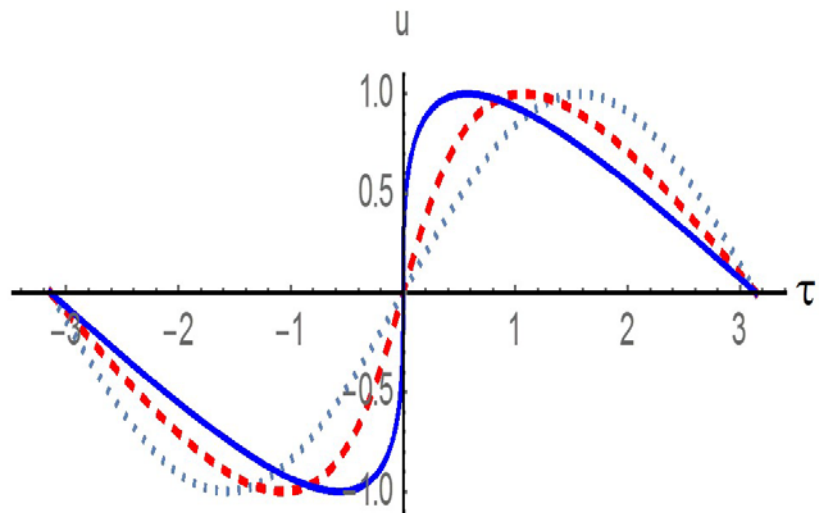
237 arising from (3.5) with $x = 0$. Let us note that the function $z(\tau, Br)$ is set in a parametric form, but
238 after expressing φ from (3.12) and substituting it in (3.11), we can obtain the explicit expression
239 for the function $\tau(z; Br)$. In the paper, we will use both explicit and implicit expressions of the
240 functions describing the moving shoreline dynamics.

241 Fig. 2 shows the moving shoreline dynamics at different wave height values in terms of the
242 breaking parameter up to the limiting value ($Br = 1$). In the limit of small parameter values, the
243 oscillations are close to sinusoidal (it is almost a linear problem). Then, with the increasing
244 amplitude, the moving shoreline velocity gets a steep leading front, while at the moving shoreline
245 vertical displacement a peculiar feature is formed at the wave run-down stage. As it is known, at
246 the time of the Riemann wave breaking, the peculiarity like $u \sim t^{1/3}$ is formed (Pelinovsky et al,
247 2013). Then, in the integral over the Riemann wave (at the moving shoreline displacement), this
248 peculiar feature will have the form $z \sim t^{4/3}$. Thus, with the wave amplitude increase, the first
249 breaking occurs at sea (at the run-down stage), and not on the coast. Then the breaking zone
250 expands and moves on to the coast, but at this stage, analytical solutions based on the Carrier-
251 Greenspan transformation become inapplicable.



252

253



254

255

256 Fig. 2. The moving shoreline dynamics (top) and its velocity (below) in the case of the incident
 257 monochromatic wave for different breaking parameter values Br (0 – the dotted line, 0.5 – the
 258 dashed line and 1 – the solid line).

259

260

4. Probabilistic characteristics of the initially sine wave run-up with a random phase

261

262

263

264

Let us now consider the probabilistic characteristics of the initially sine wave run-up with a random phase on the shore, assuming it to be uniformly distributed over the interval $[0 - 2\pi]$. These characteristics are found by using the geometric probability methods (Kendall and Stuart, 1969), so that for ergodic processes the probability density of the moving shoreline vertical

265 displacement coincides with the relative location time of the function $z(\tau)$ in the interval $(z,$
 266 $z + dz)$

$$267 \quad W(z) = \frac{1}{2\pi} \sum_{n=1}^N \left| \frac{d\tau_n}{dz} \right|, \quad (4.1)$$

268 where the summation takes place at all intersection levels $z(\tau)$. For harmonic disturbance, it is
 269 enough to restrict ourselves to considering the field on a half-period. So, for the moving shoreline
 270 vertical displacement in dimensionless variables, the derivative $d\tau/dz$ of the parametric curve
 271 (3.11) and (3.12) can be calculated through the ratio of the derivatives $d\tau/d\varphi$ and $dz/d\varphi$

$$272 \quad W_z^{\sin}(z; Br) = \frac{1}{\pi} \frac{1 + Br \sin \varphi}{\cos \varphi + Br \cos \varphi \sin \varphi} = \frac{1}{\pi \cos \varphi}, \quad (4.2)$$

273 we indicated here that the probability density depends on Br as a parameter. Finding $\cos \varphi$ from
 274 the formula (3.12) for the vertical displacement, we obtain the final expression for the probability
 275 density

$$276 \quad W_z^{\sin}(z; Br) = \frac{1}{\pi} \frac{1}{\sqrt{1 - \frac{1}{Br^2} \left[1 - \sqrt{1 + 2zBr + Br^2} \right]^2}}, \quad (4.3)$$

277 which in the linear problem for a purely sinusoidal perturbation transforms into a well-known
 278 expression for the probability distribution of a harmonic signal with a random phase (Kendall and
 279 Stuart, 1969)

$$280 \quad W_z^{\sin}(z; 0) = \frac{1}{\pi} \frac{1}{\sqrt{1 - z^2}}. \quad (4.4)$$

281 The probability distribution (4.3) for the three values of the parameter Br is shown in Fig.3.
 282 As you can see, the probability density becomes an asymmetric function with a greater probability
 283 in the area of positive values corresponding to the wave run-up on the coast than at the run-down
 284 stage. At the ends of the interval, the probability density is unlimited throughout the entire range
 285 change of Br , since the shoreline oscillations near the maximum have a zero derivative (the moving
 286 shoreline velocity in it becomes zero).

287 The obtained probability density function can be used to calculate the statistical moments
 288 of the shoreline oscillations. Technically, however, it is easier to use the parametric equations
 289 (3.11) and (3.12) and calculate all the moments.

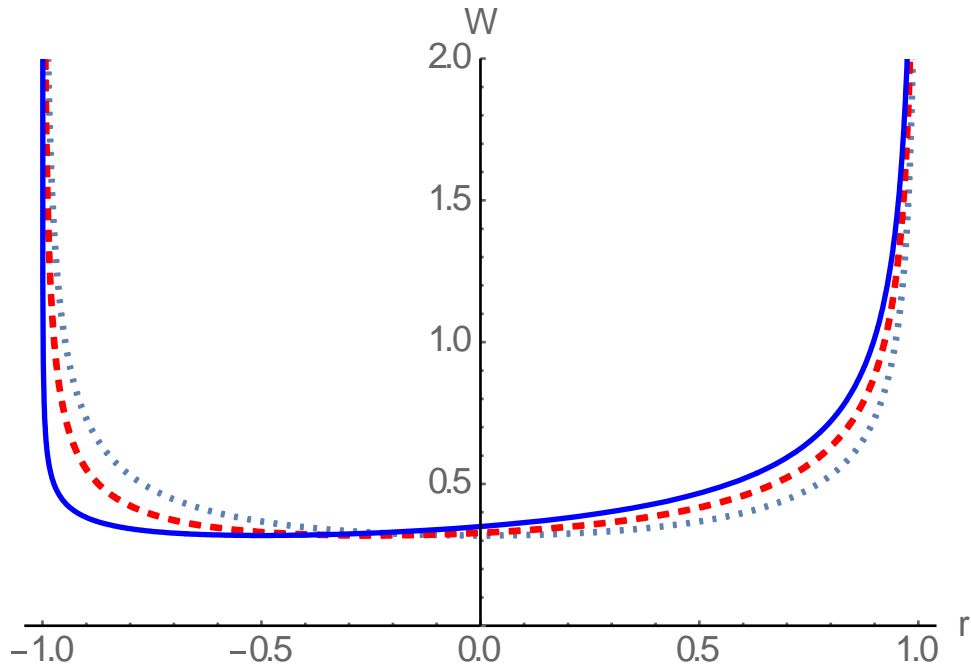
$$290 \quad M_n^z = \frac{1}{2\pi} \int_0^{2\pi} z^n(\tau) d\tau = \frac{1}{2\pi} \int_0^{2\pi} z^n(\varphi) \frac{d\tau}{d\varphi} d\varphi. \quad (4.5)$$

291 So, the first moment

$$292 \quad M_1^z = \frac{Br}{4} \quad (4.6)$$

293 determines the average water level rise on the coast when the waves approach the shore (the set-
294 up phenomenon), which is commonly observed (Dean and Walton, 2009).

295



296

297 Fig. 3. The probability density of the moving shoreline vertical displacement for the initially sine
298 wave run-up at $Br = 0$ (the dotted line), 0.5 (the dashed line) and 1 (the solid line).

299

300 The second moment determines the dispersion

$$301 \quad \delta^2 = \frac{1}{2\pi} \int_0^{2\pi} (z - M_1^z)^2 d\tau = \frac{1}{2} - \frac{3}{32} Br^2, \quad (4.7)$$

302 characterizing the fluctuation range relative to the average value; it relatively weakly decreases
303 with the growth of the parameter Br (less than 10% for non-breaking waves).

304 Finally, the total flooding time and its drainage time are easy to find from (3.11) and (3.12)
305 by finding from the equation (3.12) the value φ at which $z = 0$ and substituting the obtained values
306 in (3.11)

$$307 \quad T_{flood} = \pi - 2 \arcsin \left[\frac{\sqrt{1 + Br^2} - 1}{Br} \right] + 2\sqrt{2} \sqrt{\sqrt{1 + Br^2} - 1}, \quad (4.9)$$

308

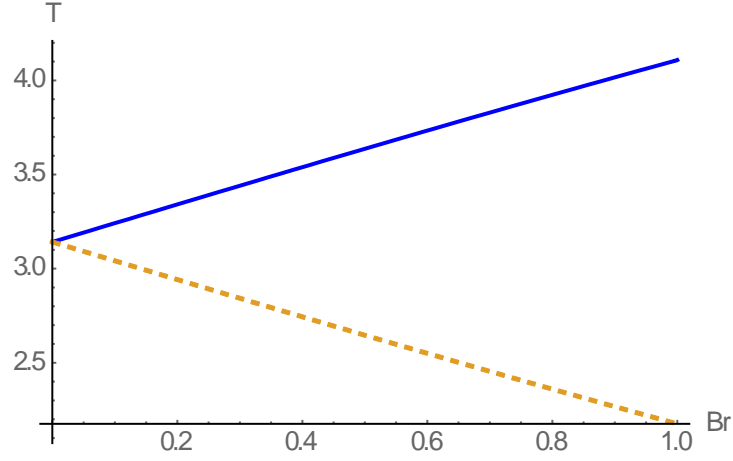
309

$$T_{dry} = \pi + 2 \arcsin \left[\frac{\sqrt{1 + Br^2} - 1}{Br} \right] - 2\sqrt{2}\sqrt{\sqrt{1 + Br^2} - 1},$$

310

Both times change almost linearly with the increasing wave amplitude (parameter Br), see Fig. 4.

311



312

Fig. 4. The total flooding time (the solid curve) and the drainage time (the dashed curve) depending on the parameter Br .

313

314

315

It is worth noting that, in contrast to the vertical displacement, the moving shoreline velocity distribution $[u = (\omega R_0 / \alpha)v]$, as it is easy to show, does not depend on the breaking parameter, and the probability density function is determined by the simple formula

316

317

318

$$W_v^{\sin}(v) = \frac{1}{\pi} \frac{1}{\sqrt{1-v^2}}. \quad (4.10)$$

319

The distribution independence on the degree of nonlinearity is well known for the Riemann waves and is explained by the compensation of compression and rarefaction areas (Gurbatov et al, 1991, 2011).

320

321

322

323

5. Probabilistic characteristics of a narrow-band wave run-up with a random amplitude and phase

324

325

Let us consider the run-up of a quasi-harmonic wave with a random amplitude and phase on a flat slope. To do this, we will first rewrite the formulas (4.3) and (4.10) for them to include the wave amplitude. It is convenient to enter the maximum height R_{max} as the amplitude scales at which the breaking parameter turns into 1

326

327

328

329

$$Br = \frac{\omega^2 R_{max}}{\alpha^2 g} = 1, \quad (5.1)$$

330 and to use the dimensionless displacement ($y=r/R_{max}$). Then the dimensionless amplitude is

$$331 \quad A = \frac{R_0}{R_{max}} \leq 1, \quad (5.2)$$

332 and the formula (4.3) is converted to the form ($-A < y < A$)

$$333 \quad W_y^{\sin}(y; A) = \frac{1}{\pi} \frac{1}{\sqrt{A^2 - \left[1 - \sqrt{1 + 2y + A^2}\right]^2}}. \quad (5.3)$$

334 Assuming now that the wave amplitude A is a random variable, we average (5.3) by using
335 the amplitude distribution density $W_A(A)$

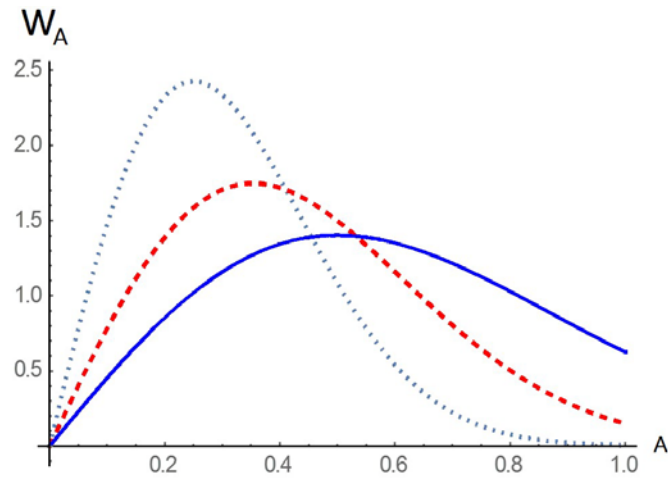
$$336 \quad W(y) = \int_y^{\infty} W_y^{\sin}(y; A) W_A(A) dA. \quad (5.4)$$

337 The formula (5.4) has an important practical meaning: by the measured distribution of the wave
338 amplitudes far from the coast (re-computed on run-up amplitudes in the linear theory), it is possible
339 to obtain the distribution of the wave run-up characteristics on the coast. The only requirement
340 imposed on the wave ensemble is that it should not contain breaking waves, which should be
341 somehow removed from the record. It immediately follows that the Gaussian field containing large
342 amplitude tails does not fit this requirement, and it should be modified. Therefore, we assume the
343 amplitude distribution to be finite for $A < A_{max} = 1$. The narrow-band random wave field contains
344 sine waves with almost constant frequency and random amplitude and phase. It means that if the
345 wave amplitude is below the “breaking amplitude” $A_{max} = 1$, the breaking will not be implemented
346 in any way, and the random wave run-up will take place without any breaking. Further calculations
347 depend on the specific type of the amplitude distribution.

348 Let us construct the finite amplitude distribution at which the linear field distribution is
349 close to the Gaussian form and modify the Rayleigh distribution for wave heights in the area
350 $A < A_{max} = 1$ (Fig. 5)

$$351 \quad W_A(A; A_{max}, A_s) = \frac{1}{1 - \exp(-2A_{max}^2 / A_s^2)} \frac{4A}{A_s^2} \exp\left(-2\frac{A^2}{A_s^2}\right), \quad A \leq A_{max}, \quad (5.5)$$

352 to make the density function distribution normalized. Here, A_s is the so-called significant wave
353 run-up height (an averaged value of 1/3 highest amplitudes). We would like to note here, that it
354 follows from (2.11) and (2.12) that the extremal run-up characteristics in the nonlinear theory
355 remain the same as in the linear theory. This means that the significant wave run-up height remains
356 the same as in the nonlinear theory.



357

358 Fig. 5. The modified Rayleigh distribution (5.5) for different distribution values A_s/A_{max} ;
 359 0.5 – the dotted curve, 0.7 – the dashed line, 1 – the solid line.

360

361 When $A_s \ll A_{max} = I$, the distribution (5.5) transforms into the Rayleigh one, which is
 362 characteristic of the Gaussian initial distribution of a narrow-band random signal. With the help of
 363 (5.5), it becomes possible to calculate the distribution function of shoreline oscillations for the
 364 various wave energy. So, with the incident wave small amplitude ($A_s \ll I$), the distribution (5.3)
 365 can be replaced by a simpler expression (4.4) and the answer is the run-up distribution
 366 characteristics in the linear theory:

$$367 \quad W_{lin}(y; A_{max}, A_s) = \frac{4}{\pi A_s^2 [1 - \exp(-2A_{max}^2 / A_s^2)]} \int_y^{A_{max}} \frac{A}{\sqrt{A^2 - y^2}} \exp\left(-2 \frac{A^2}{A_s^2}\right) dA. \quad (5.6)$$

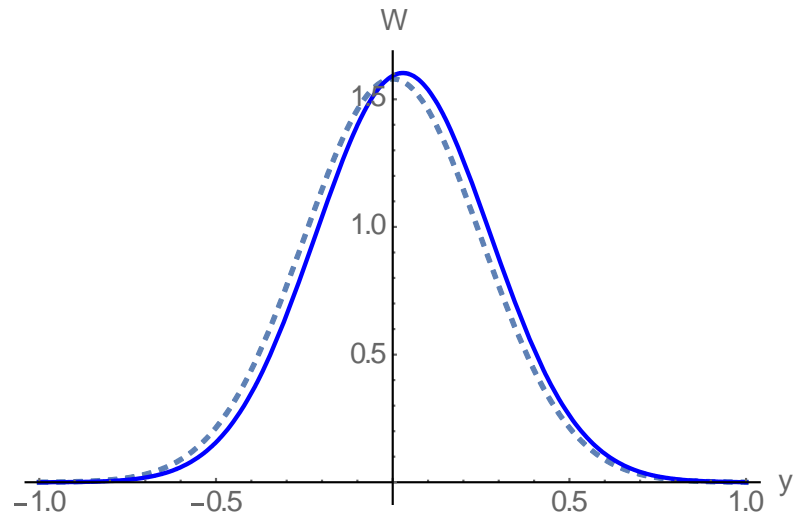
368 Besides, if $A_s \ll A_{max} = I$, the integral (5.6) is reduced to the Gaussian distribution

$$369 \quad W_{lin}(y; A_s) = \frac{2}{\sqrt{2\pi} A_s} \exp\left(-2 \frac{y^2}{A_s^2}\right), \quad (5.7)$$

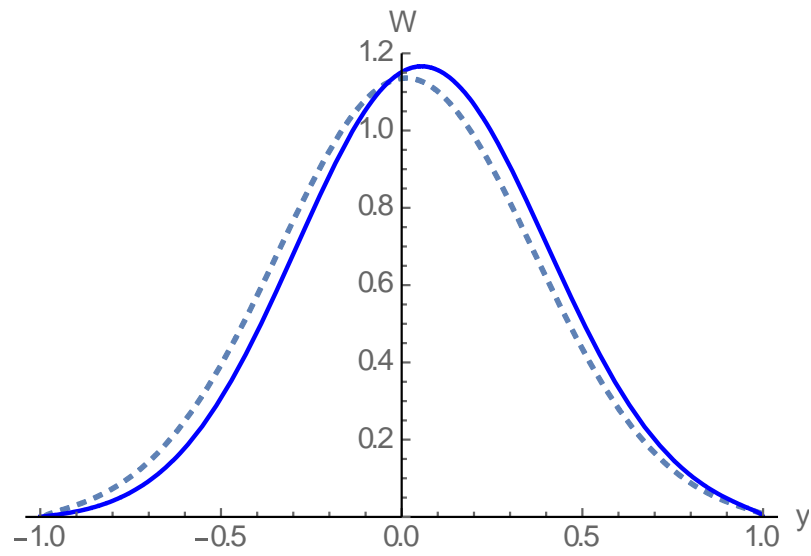
370 where, $A_s = 2\sigma_y$, and σ_y^2 is the moving shoreline oscillation dispersion.

371 Fig. 6 shows the distribution of the run-up characteristics for different ratios of A_s/A_{max}
 372 values by the formulas (5.4) and (5.5); they are shown in solid lines. Here the dashed lines show
 373 the calculation results according to the linear theory (5.6). As one can see, with $A_s/A_{max} = 0.5$ (the
 374 top panel) and 0.7 (the middle panel), the linear distribution is close to the Gaussian one.
 375 Nonlinearity leads to the asymmetry of the distribution function density in the direction of positive
 376 values corresponding to the wave characteristics on the coast. If the undisturbed wave ensemble is
 377 made of relatively large waves ($A_s/A_{max} = 1$), their distribution is far from the Gaussian, both in the
 378 linear and in the nonlinear approximation.

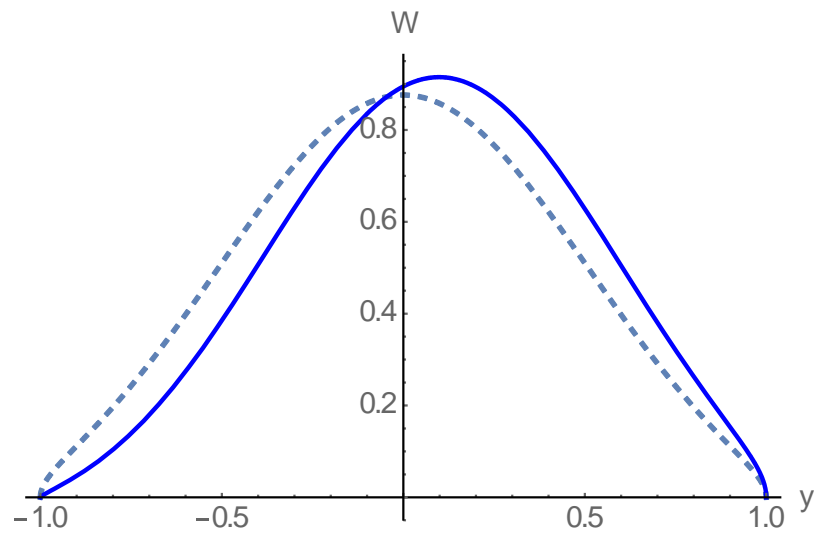
379



380



381



382

383

384

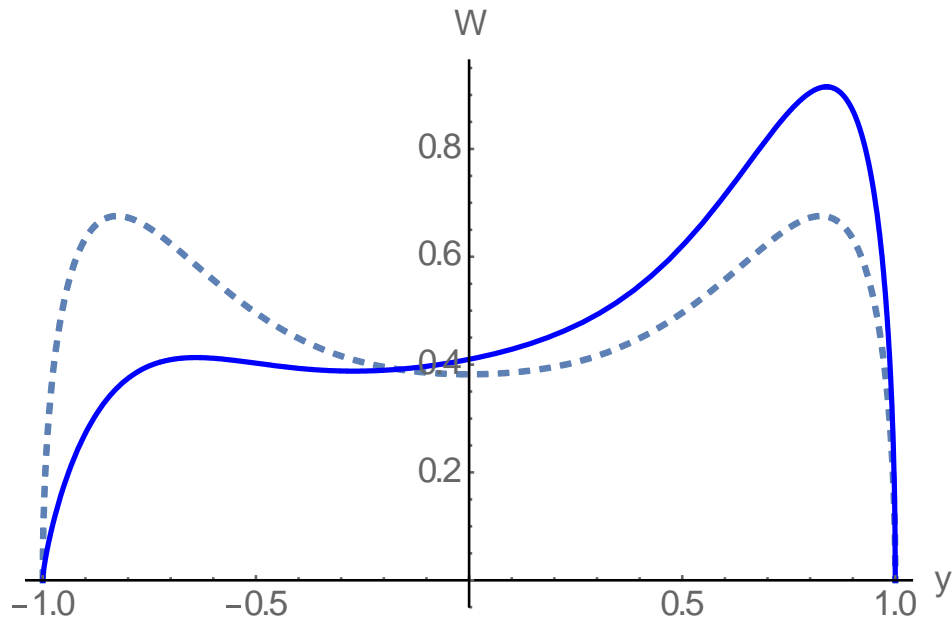
385

Fig. 6. The probabilistic density function of the vertical shoreline displacement in the nonlinear theory (the solid lines) and in the linear theory (the dashed lines) for different A_s/A_{max} values: (the upper panel), 0.7 (the middle panel) and 1 (the lower panel).

386 The finite ($A < A_{max}$) power-law distribution concentrated mainly near the maximum
 387 amplitude A_{max} can be considered to be another example of undisturbed large-amplitude waves.

388
$$W_A(A) = \frac{6A^5}{A_{max}^6}. \quad (5.8)$$

389 Fig. 7 shows the graphs of the probabilistic density function of the moving shoreline displacement
 390 calculated by using the formulas (5.4) and (4.4) in the linear theory and (5.3) in the nonlinear
 391 theory. It is also seen in the figure, the nonlinear effects lead to a strong asymmetry towards the
 392 positive values, that is, to the wave amplification at the run-up up stage than at the run-down stage.



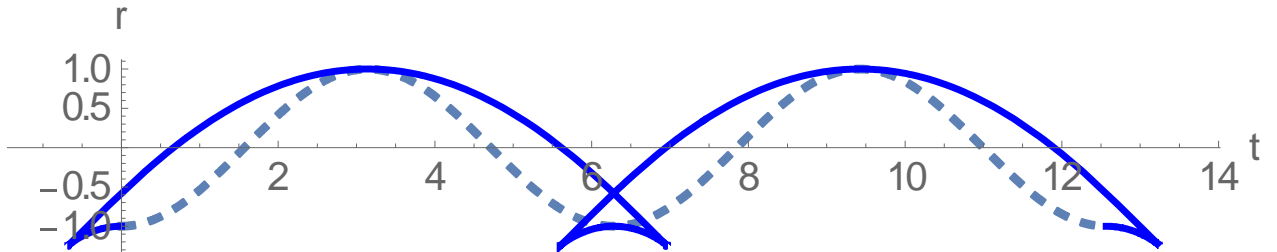
393
 394 Fig. 7. The probabilistic density function of the shoreline vertical displacement in the linear
 395 theory (the dashed line) and non-linear theory (the solid line)

396

397 **6. The wave breaking effect on probabilistic run-up characteristics**

398 The theory described above is valid for non-breaking waves. The mentioned wave ensemble,
 399 strictly speaking, cannot be the Gaussian one, as it always has unlimited tails in the probability
 400 density function. Let us briefly discuss what the formulas obtained for non-breaking waves lead
 401 to in the presence of broken waves. Fig. 8 shows the parametric curve (3.11) - (3.12) when $Br =$
 402 2. Formally, the curve became multi-valued in the range of negative values corresponding to the
 403 maximum water outflow from the coast. We have already indicated that the probability density
 404 function of the moving shoreline vertical displacement $W(\xi)$ coincides with the relative residence
 405 time $\xi(t)$ of the function in the interval $(\xi, \xi + d\xi)$, which is calculated by the formula (3.1). In
 406 contrast to negative cut-off bias values, in the area of positive values there is no ambiguity, and,

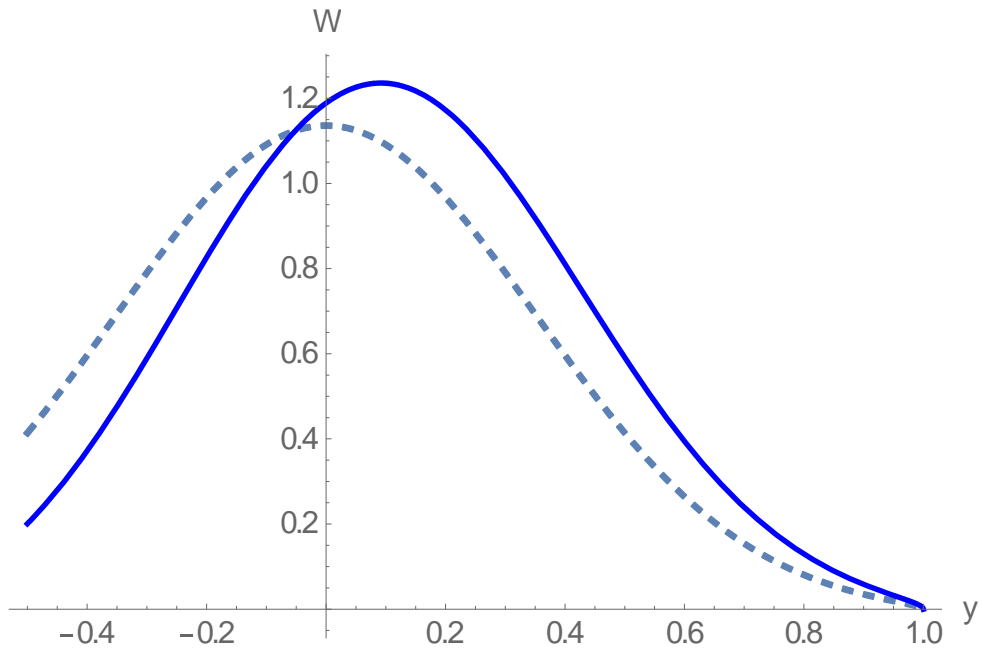
407 therefore, all the calculations can be carried out by using the formulas described above. The
 408 calculation example with $Br = 2$ and $r > -0.5$ (in the zone of one-value solution) is shown in Fig. 9.
 409 However, these results should be treated with caution. If $Br > 1$ the Jacobian breaks down seawards
 410 of the shoreline. This may affect the probabilistic distribution on the positive side. This important
 411 issue requires going beyond the theory discussed in this article.



412
413

414 Fig. 8. The parametric curve (3.11) - (3.12) with $Br = 2$ (the solid curve) in comparison with the
 415 linear problem with $Br = 0$ (the dashed line)

416



417

418 Fig. 9. The probability density function at $Br = 2$, constructed by the formulas (5.3), (5.4) and (5.5)
 419 (the solid line) in comparison with the linear distribution (5.6) (the dotted line). $A/A_{max} = 0.7$.

420

421 7. Discussion and conclusion

422 In this paper, we study the run-up of irregular narrow-band waves with a random envelope
 423 (swell, storm surges, and tsunami) on a beach of a constant slope. The work was carried out in the
 424 framework of the nonlinear wave theory with one important assumption: there should be no

425 breaking waves in the wave ensemble. This restriction is quite strict for field and laboratory
426 conditions, but nevertheless, there are cases when it is performed. For instance, 75% of historical
427 tsunami waves climbed on the coast with no breaking (Mazova et al, 1983). In the experiments
428 performed in the Warwick University tank and in the Large Tank in Hannover (Denissenko et al,
429 2011, 2013), this condition was fulfilled.

430 The wave nonlinearity at the run-up stage leads to increased deviations from Gaussianity, as might
431 be expected from general considerations. Nevertheless, it is shown that the probability distribution
432 of the moving shoreline velocity does not depend on the wave nonlinearity and can be calculated
433 within the linear theory framework. The same conclusion can be drawn about the distribution of
434 the extreme run-up characteristics (the moving shoreline displacement and speed), which, in fact,
435 has already been discussed earlier (Didenkulova et al, 2008). However, the probabilistic density
436 function of the moving shoreline displacement differs from that predicted one in the linear theory
437 framework. It is described by the formula (5.4) by using either the theoretical or the measured
438 distribution of the incident wave amplitudes. The paper gives the calculation results of the
439 probabilistic run-up characteristics with the modified Rayleigh distribution for wave amplitudes.

440 The wave breaking leads to the inapplicability of the wave run-up theory based on the
441 Carrier-Greenspan transformation. If, nevertheless, the share of large amplitude waves is small,
442 the breaking occurs mainly at the run-down stage, having little effect on the long-wave coastal
443 flooding characteristics (see Section 6). This question, however, requires a special study based on
444 direct numerical solutions of the shallow-water equations or their nonlinear-dispersive
445 generalizations.

446 Finally, it is worth noting that we considered the narrow-band wave run-up with a random
447 amplitude and phase. As far as the random waves with a wide spectrum are concerned, they may
448 be the problem of further consideration.

449 The obtained probability density functions of the vertical displacement of the moving
450 shoreline are useful to compute statistical characteristics of flooding time and force on coasts and
451 constructions, which are necessity for the mitigation of natural marine hazards.

452 Now in practice various generalizations of shallow-water equations are used to analyze
453 tsunami run-up including the wave dispersion, see for instance (Lovholt et al, 2012). The wave
454 dispersion is a quadratic dissipative term that prevents us from getting analytical results, so its
455 influence on statistical characteristics should be investigated in the future.

456

457 **Acknowledgment:**

458 The work is supported by the grants from the Russian Science Foundation: No.19-12-00256 (in
459 part of computing the random Riemann wave characteristics) and No. 16-17-00041 (in part of
460 computations the probability density function of the moving shoreline).

461

462 **References**

463

- 464 1. Anderson, D., Harris, M., Hartle, H., Nicolsky, D., Pelinovsky, E., Raz, A. and Rybkin, A.:
465 Runup of long waves in piecewise sloping U-shaped bays, *Pure and Applied Geophysics*, 174,
466 3185-3207, 2017.
- 467 2. Antuano, M. and Brocchini, M.: Maximum run-up, breaking conditions and dynamical forces
468 in the swash zone: a boundary value approach, *Coastal Engineering*, 55, 732-730, 2008.
- 469 3. Antuano, M. and Brocchini, M.: Solving the nonlinear shallow-water equations in physical
470 space, *J. Fluid Mech.*, 643, 207–232, 2010.
- 471 4. Aydin. B. and Kanoglu, U.: New analytical solution for nonlinear shallow water-wave
472 equations, *Pure and Applied Geophysics*, 174, 3209–3218, 2017.
- 473 5. Bec, J. and Khanin, K.: Burgers turbulence, *Physics Reports*, 447, 1-66, 2007.
- 474 6. Burgers, J. M.: *The Nonlinear Diffusion Equation*. Dordrecht, D. Reidel, 1974.
- 475 7. Carrier, G.F.: On-shelf tsunami generation and coastal propagation. In *Tsunami: Progress in*
476 *Prediction, Disaster Prevention and Warning*, eds. Tsuchiya, Y. & Shuto, N. Kluwer, Dordrecht,
477 1-20, 1995.
- 478 8. Carrier, G.F. and Greenspan, H.P.: Water waves of finite amplitude on a sloping beach,
479 *J. Fluid Mech.*, 4.97–109, 1958.
- 480 9. Carrier, G.F., Wu, T.T. and Yeh, H.: Tsunami run-up and draw-down on a plane beach, *Journal*
481 *of Fluid Mechanics*, 475, 79-99, 2003.
- 482 10. Choi, J., Kwon, K.K. and Yoon, S.B.: Tsunami inundation simulation of a built-up area using
483 equivalent resistance coefficient, *Coastal Engineering Journal*, 54, 1250015 (25 pages), 2012.
- 484 11. Dean, R.G. and Walton, T.L.: Wave setup. In: Kim, Y.C. (Ed.), *Handbook of Coastal and Ocean*
485 *Engineering*. World Sci, Singapore, 2009.
- 486 12. Denissenko, P., Didenkulova, I., Pelinovsky, E. and Pearson J.: Influence of the nonlinearity
487 on statistical characteristics of long wave runup, *Nonlinear Processes in Geophysics*, 18, 967-
488 975, 2011.
- 489 13. Denissenko, P., Didenkulova, I., Rodin, A., Listak, M. and Pelinovsky E.: Experimental
490 statistics of long wave runup on a plane beach, *Journal of Coastal Research*, 65, 195-200, 2013.

- 491 14.Didenkulova, I.: New trends in the analytical theory of long sea wave runup. In: Applied Wave
492 Mathematics: Selected Topics in Solids, Fluids, and Mathematical Methods (Ed: E. Quak and
493 T. Soomere). Springer, 265–296, 2009.
- 494 15.Didenkulova, I., Pelinovsky, E. and Sergeeva, A.: Runup of long irregular waves on plane
495 beach. In: Extreme Ocean Waves (Eds: Pelinovsky E., Kharif C.), Springer, 83-94, 2008.
- 496 16.Didenkulova, I.I., Sergeeva, A.V., Pelinovsky, E.N. and Gurbatov, S.N.: Statistical estimates
497 of characteristics of long wave run up on the shore, Izvestiya, Atmospheric and Oceanic
498 Physics, 46, 530–532, 2010.
- 499 17.Didenkulova, I., Pelinovsky, E. and Sergeeva, A.: Statistical characteristics of long waves
500 nearshore, Coastal Engineering, 58, 94-102, 2011.
- 501 18.Dobrokhotov, S.Yu.,Minenkov, D.S., Nazaikinskii, V.E. and Tirozzi, B.: Simple exact and
502 asymptotic solutions of the 1D run-up problem over a slowly varying (quasiplanar) bottom. In
503 Theory and Applications in Mathematical Physics, World Scientific, Singapore, 29-47, 2015.
- 504 19.Frisch, U.: Turbulence: the legacy of A. N. Kolmogorov, Cambridge University Press, 1995.
- 505 20.Frisch, U. and Bec, J.: Burgulence. In: New trends in turbulence (Eds: M. Lesieur, A.Yaglom
506 and F. David), Springer EDP-Sciences, 341–383, 2001.
- 507 21.Gurbatov, S. N., Saichev, A. I. and Shandarin, S. F.: Large-scale structure of the Universe. The
508 Zeldovich approximation and the adhesion model, Physics Uspekhi, 55, 223–249, 2012.
- 509 22.Gurbatov, S.N., Malakhov, A.N. and Saichev, A.I.: Nonlinear Random Waves and Turbulence
510 in Nondispersive Media: Waves, Rays, Particles. Manchester University Press, 1991.
- 511 23.Gurbatov, S.N., Rudenko, O.V. and Saichev, A.I.: Waves and Structures in Nonlinear
512 Nondispersive Media. Berlin, Heidelberg: Springer-Verlag, and Beijing: Higher Education
513 Press, 2011.
- 514 24.Gurbatov, S.N. and Saichev, A.I.: Inertial nonlinearity and chaotic motion of particle fluxes,
515 Chaos, 3, 333-358, 1993.
- 516 25.Gurbatov, S., Simdyankin, S., Aurell, E., Frisch, U. and Toth, G.: On the decay of Burgers
517 turbulence, J. Fluid Mech., 344, 349-374, 1997.
- 518 26.Gurbatov, S.N., Deryabin, M.S., Kasyanov, D.A. and Kurin, V.V.: Evolution of narrow-band
519 noise beams for large acoustic Reynolds numbers, Radiophysics and Quantum Electronics, 61,
520 478–490, 2018.
- 521 27.Gurbatov, S., Deryabin, M., Kurin, V. and Kasyanov, D.: Evolution of intense narrowband
522 noise beams, Journal of Sound and Vibration, 439, 208-218, 2019.

- 523 28.Harris, M.W., Nicolsky, D.J., Pelinovsky, E.N. and Rybkin A.V.: Runup of nonlinear long
524 waves in trapezoidal bays: 1-D analytical theory and 2-D numerical computations, *Pure and*
525 *Applied Geophysics*, 172, 885-899, 2015.
- 526 29.Harris, M.W., Nicolsky, D.J., Pelinovsky, E.N., Pender, J.M. and Rybkin, A.V.: Run-up of
527 nonlinear long waves in U-shaped bays of finite length: Analytical theory and numerical
528 computations, *J Ocean Engineering and Marine Energy*, 2, 113-127, 2016.
- 529 30.Hughes, M.G., Moseley, A.S. and Baldock, T.E.: Probability distributions for wave runup on
530 beaches, *Coastal Engineering*, 57, 575-584, 2010.
- 531 31.Huntley, D.A., Guza, R.T. and Bowen, A.J.: A universal form for shoreline run-up spectra, *J.*
532 *Geophys. Res.*, 82, 2577–2581, 1977.
- 533 32.Kaiser, G., Scheele, L., Kortenhaus, A., Lovholt, F., Romer, H. and Leschka, S.: The influence
534 of land cover roughness on the results of high resolution tsunami inundation modeling, *Nat.*
535 *Hazards Earth Syst. Sci.*, 11, 2521–2540, 2011.
- 536 33.Kendall, M.G. and Stuart, A.: *The Advanced Theory of Statistics. Volume I. Distribution*
537 *Theory*. London. 1969.
- 538 34.Kian, R., Velioglu, D., Yalciner, A.C. and Zaytsev, A.: Effects of harbor shape on the induced
539 sedimentation; L-type basin, *Journal of Marine Science and Engineering*, 4, 55-65, 2016.
- 540 35.Løvholt, F., Pedersen, G., Bazin, S., Kühn, D., Bredesen, R.E., and Harbitz, C.: Stochastic
541 analysis of tsunami runup due to heterogeneous coseismic slip and dispersion, *J. Geophys. Res.*,
542 117, C03047, 2012. doi: 10.1029/2011JC007616.
- 543 36.Macabuag, J., Rossetto, T., Ioannou, I., Suppasri, A., Sugawara, D., Adriano, B., Imamura, F.,
544 Eames, I. and Koshimura, S.: A proposed methodology for deriving tsunami fragility functions
545 for buildings using optimum intensity measures, *Nat Hazards*, 84, 1257–1285, 2016.
- 546 37.Madsen, P.A. and Fuhrman, D.R.: Run-up of tsunamis and long waves in terms of surf-
547 similarity, *Coast. Eng.*, 55, 209–223, 2008.
- 548 38.Madsen, P. and Schaffer, H. A.: Analytical solutions for tsunami runup on a plane beach: single
549 waves, N-waves and transient waves, *J. Fluid Mech.*, 645, 27-57, 2010.
- 550 39.Mazova, R.Kh., Pelinovsky, E.N. and Solov'yev, S.L.: Statistical data on the tsunami runup
551 onto shore, *Oceanology*, 23, 698 – 702, 1983.
- 552 40.Molchanov, S.A., Surgailis, D. and Woyczynski, W.A.: Hyperbolic asymptotics in Burgers’
553 turbulence and extremal processes, *Comm. Math. Phys.*, 168, 209-226, 1995.
- 554 41.Ozer, S.C., Yalciner, A.C. and Zaytsev, A.: Investigation of tsunami hydrodynamic parameters
555 in inundation zones with different structural layouts, *Pure and Applied Geophysics*, 172, 931–
556 952, 2015a.

- 557 42.Ozer, S.C., Yalciner, A.C., Zaytsev, A., Suppasri, A. and Imamura, F.: Investigation of
558 hydrodynamic parameters and the effects of breakwaters during the 2011 Great East Japan
559 Tsunami in Kamaishi Bay, *Pure and Applied Geophysics*, 172, 3473–3491, 2015b.
- 560 43.Park, H., Cox, D.T. and Barbosa, A.R.: Comparison of inundation depth and momentum flux
561 based fragilities for probabilistic tsunami damage assessment and uncertainty analysis, *Coastal*
562 *Eng.*, 122, 10–26, 2017.
- 563 44.Pelinovsky, E. and Mazova, R.: Exact analytical solutions of nonlinear problems of tsunami
564 wave run-up on slopes with different profiles, *Nat. Hazards*, 6, 227–249, 1992.
- 565 45.Pelinovsky, D., Pelinovsky, E., Kartashova, E., Talipova, T. and Giniyatullin, A.: Universal
566 power law for the energy spectrum of breaking Riemann waves, *JETP Letters*, 98, 237-241,
567 2013.
- 568 46.Pedersen, G.: Fully nonlinear Boussinesq equations for long wave propagation and run-up in
569 sloping channels with parabolic cross sections, *Natural Hazards*, 84, S599–S619, 2016.
- 570 47.Qi, Z.X, Eames, I. and Johnson E.R.: Force acting on a square cylinder fixed in a free-surface
571 channel flow, *J Fluid Mech*, 756, 716–727, 2014.
- 572 48.Raz, A., Nicolsky, D., Rybkin, A. and Pelinovsky, E.: Long wave run-up in asymmetric bays
573 and in fjords with two separate heads, *Journal of Geophysical Research – Oceanus*, 123, 2066-
574 2080, 2018.
- 575 49.Rudenko, O.V. and Soluyan S.I.: *Nonlinear Acoustics*. Pergamon Press, NY, 1977.
- 576 50.Rybkin, A. Pelinovsky, E.N. and Didenkulova, I.: Nonlinear wave run-up in bays of arbitrary
577 cross-section: generalization of the Carrier-Greenspan approach, *J Fluid Mechanics*, 748, 416-
578 432, 2014.
- 579 51.Shimozono, T.: Long wave propagation and run-up in converging bays, *J. Fluid Mech.*, 798,
580 457-484, 2016.
- 581 52.Synolakis, C.E.: The runup of solitary waves, *J. Fluid Mech.*, 185, 523–545, 1987.
- 582 53.Synolakis, C., Bernard, E.N., Titov, V.V., Kanoglu, U. and Gonzalez, F.I.: Validation and
583 verification of tsunami numerical models, *Pure and Applied Geophysics*, 165, 2197-2228,
584 2008.
- 585 54.Tinti, S. and Tonini, R.: Analytical evolution of tsunamis induced by near-shore earthquakes
586 on a constant-slope ocean, *J. Fluid Mech.*, 535, 33–64, 2005.
- 587 55.Woyczynski, W.A.: *Burgers–KPZ Turbulence*. Gottingen Lectures, Berlin, Springer-Verlag,
588 1998.

589 56.Xiong, Y., Liang, Q., Park, H., Cox, D. and Wang, G.: A deterministic approach for assessing
590 tsunami-induced building damage through quantification of hydrodynamic forces, Coastal
591 Engineering, 144, 1-14, 2019.
592